PHYSICAL REVIEW C VOLUME 43, NUMBER 5 MAY 1991

Binding energy and momentum distribution of nuclear matter using Green's function methods

A. Ramos
TRIUMF, 4004 Wesbrook Mall, Vancouver, British Columbia, Canada V6T 2A3

W. H. Dickhoff
Department of Physics, Washington University, St. Louis, Missouri 63130

A. Polls
Departament d'Estructura i Constituents de la Matèria, Universitat de Barcelona, E-08028 Barcelona, Spain
(Received 2 July 1990)

The influence of hole-hole (h-h) propagation in addition to the conventional particle-particle (p-p) propagation, on the energy per particle and the momentum distribution is investigated for the v_2 central interaction which is derived from Reid's soft-core potential. The results are compared to Brueckner-Hartree-Fock calculations with a continuous choice for the single-particle (SP) spectrum. Calculation of the energy from a self-consistently determined SP spectrum leads to a lower saturation density. This result is not corroborated by calculating the energy from the hole spectral function, which is, however, not self-consistent. A generalization of previous calculations of the momentum distribution, based on a Goldstone diagram expansion, is introduced that allows the inclusion of h-h contributions to all orders. From this result an alternative calculation of the kinetic energy is obtained. In addition, a direct calculation of the potential energy is presented which is obtained from a solution of the ladder equation containing p-p and h-h propagation to all orders. These results can be considered as the contributions of selected Goldstone diagrams (including p-p and h-h terms on the same footing) to the kinetic and potential energy in which the SP energy is given by the quasiparticle energy. The results for the summation of Goldstone diagrams leads to a different momentum distribution than the one obtained from integrating the hole spectral function which in general gives less depletion of the Fermi sea. Various arguments, based partly on the results that are obtained, are put forward that a self-consistent determination of the spectral functions including the p-p and h-h ladder contributions (using a realistic interaction) will shed light on the question of nuclear saturation at a nonrelativistic level that is consistent with the observed depletion of SP orbitals in finite nuclei.

I. INTRODUCTION

In spite of the considerable effort devoted to the microscopic description of nuclear matter, none of the methods based on nonrelativistic dynamics and two-body interactions, such as Brueckner theory,[1-3] the variational approach,[4,5] the coupled-cluster scheme,[6] or Monte Carlo techniques,[7] is able to reproduce satisfactorily the nuclear matter saturation properties, namely, an average binding energy per nucleon $B=-16$ MeV at an equilibrium density $\rho_0=0.17$ fm^{-3}. If for a given interaction the equilibrium density is well predicted, then the binding energy per nucleon is underestimated whereas when the binding energy is correctly reproduced, the saturation density turns out to be too high. This results in the so-called Coester band in which the saturation point of a given interaction is correlated with the strength of the tensor force. The stronger the tensor force the lower the saturation density.

Relativistic many-body theory[8-10] represents an alternative description to explain nuclear saturation. However, the results are rather sensitive to the coupling to negative-energy states (vacuum polarization effects).[11] It has been observed that it fails to provide sufficient binding in finite nuclei.[12] More seriously, it has recently been shown that the relativistic approaches lead to a very small depletion of the Fermi sea.[13] This small depletion is not consistent with the experimental results that are becoming available from $(e,e'p)$ experiments performed at NIKHEF.[14,15]

It has been shown, on the other hand, that corrections due to suppressed degrees of freedom in the nonrelativistic many-body theory based on two-body interactions, can be cast in the form of a small three-body force, either phenomenological[16] or having a more fundamental origin,[17] providing an alternative description of nuclear saturation. It is therefore necessary to have a reliable and well controlled description of nuclear matter at the level of two-body interactions to which the corrective effects of three-body forces are subsequently applied.

It is the purpose of this paper to investigate whether an improved and more consistent treatment of the many-body system, still based on nonrelativistic dynamics and two-body forces, can provide new information on the saturation problem of nuclear matter. We shall pay special attention to connect the properties of a particle in the

medium, contained in the single-particle (SP) self-energy, with the resulting effective two-body interaction, using the formalism of Green's functions.[18] Since the SP self-energy, describing the modified properties of a particle in the medium (dressed particle), is determined from the two-body effective interaction between dressed particles, and this requires, in turn, the knowledge of the propagator (related to the self-energy through the Dyson equation), we are dealing with a coupled problem which must be solved self-consistently. A self-consistent treatment of the Green's functions formalism leads to the so-called self-consistent Green's function (SCGF) theory.[19–21]

In Sec. II we start reviewing the SCGF method in the ladder approximation and subsequently present the four different methods which are compared in this paper. First, we summarize in Sec. II A an initial step[19,20] to a complete self-consistent solution in which self-consistency is only required for the real part of the on-shell self-energy (the quasiparticle energy). This method, which will be referred to as the particle-particle–hole-hole (PPHH) calculation, treats the hole-hole (h-h) correlations in the ladder equation for the effective interaction on the same footing as the familiar particle-particle (p-p) propagation considered in Brueckner-type calculations. Using the self-consistent SP spectrum this method yields the PPHH estimate of the energy per particle.

Additional information can be obtained by solving the Dyson equation including the complete energy dependence of both the real and imaginary parts of the self-energy after the quasiparticle energy is determined self-consistently according to the PPHH scheme. This leads to results for the dressed propagators in terms of the spectral functions of the correlated system, which in turn determine the momentum distribution. Moreover, for the case of a two-body interaction, this dressed SP propagator also determines the binding energy of the system in terms of separate contributions from the kinetic and potential energy for the interacting system. The basic equations for this dressed propagator method (DP calculation) are presented in Sec. II B. It should be noted that the results for the dressed propagator can be considered as the first iteration for the complete solution in which the SP propagator itself is determined self-consistently.

For the purpose of later comparisons, a third method (PP calculation) is briefly summarized in Sec. II C, namely, the lowest order in the Bethe-Brueckner expansion for the binding energy. This includes only the contribution of p-p propagation in the ladder equation but treats the SP energy as in the PPHH method which leads to a continuous SP spectrum across k_F. In Sec. II D we present a fourth method, which represents a novel approximation of the binding energy as separate expansions for the kinetic and potential energy in terms of Goldstone p-p and h-h ladder diagrams (GE calculation).

It is important to note that we are not aiming at a definite answer on the saturation problem of nuclear matter. The approximations discussed in this paper involve h-h propagation to all orders and in this sense they all go beyond the concept of the hole-line expansion. As far as the binding energy is concerned, Day's three hole-line calculation and four hole-line estimate,[22] has to be regarded as a much more complete result in the context of the hole-line expansion. For example, Day's results include three-body cluster terms whereas the ladder structure of our approximations generates only two-body cluster diagrams, even if h-h propagation is considered to all orders. However, one aim of the present investigations is to establish whether a symmetrical treatment of particle and holes which can lead to quantum coherence (like in pairing), can provide new information on the validity of the hole-line expansion. Moreover, the techniques used in this paper are based on Green's function theory and allow the study of various other properties of nuclear matter apart from the binding energy, due to specific correlations in a natural and systematic way. In particular, the ladder approach discussed in this paper amounts to treating the influence of short-range correlations.

Results for the momentum distribution and binding energy of nuclear matter are presented and compared in Sec. III. Treating particles and holes symmetrically, as implied by the Green's functions formalism, leads to the appearance of complex solutions (pairing instabilities)[23] if the interaction is attractive enough, indicating that the system prefers a superfluid-type solution. A strong pairing instability has been found for the $^3S_1$-$^3D_1$ channel of the Reid potential and, therefore, an extended description,[24–26] which allows for the treatment of the pairing features of Fermi systems in the same SCGF scheme, has to be adopted.[27] To avoid this problem the methods described in Sec. II have been applied using the homework v_2 interaction, which is the central part of the Reid's soft-core potential[28] in the $^3S_1$-$^3D_1$ channel, allowed to operate in all partial waves. Although the P-wave component of the v_2 interaction gives rise to a weak pairing instability,[21] it is weak enough to still allow a reliable numerical calculation assuming a normal Fermi system. We choose this interaction also because results can be compared to other calculations,[22,29–31] which were mainly aimed at clarifying the discrepancies between the variational and the Brueckner results. We note, however, that some results obtained with the v_2 interaction might not be relevant for the properties of realistic nuclear matter.

The momentum distribution results presented in Sec. III correspond to two different methods. One is obtained from the dressed propagator used in Sec. II B, by integrating the corresponding hole spectral function $S_h(k,\omega)$ over all possible excited states. The other corresponds to the expansion in terms of Goldstone p-p and h-h ladder diagrams presented in Sec. II D which can be summed by taking the derivative of the self-energy at the quasiparticle energy. There are noticeable differences between these two methods which should be further investigated.

Finally, Sec. IV contains a summary and conclusions.

II. SELF-CONSISTENT GREEN'S FUNCTION METHOD IN THE LADDER APPROXIMATION

In a correlated many-body system, the properties of a particle are modified with respect to those in free space as a result of its interactions with the other particles. Cor-

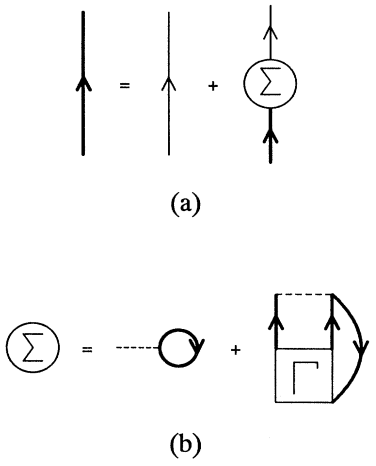

FIG. 1. Diagrammatic representation of the Dyson equation (a) for the dressed SP propagator (thick line). The structure of the proper self-energy is given in (b), where the coupling to the vertex function Γ is shown. The bare interaction, represented by the dotted line, contains both direct and exchange terms.

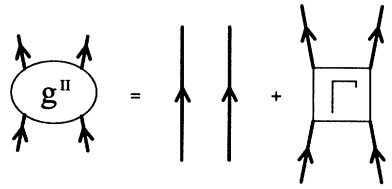

FIG. 2. Diagrammatic representation of the two-body propagator. The first diagram, which implicitly contains also the exchange term, represents the propagation of two dressed particles without interacting with each other. The second diagram represents all possible interactions between dressed propagators and defines the vertex function Γ.

respondingly, the interaction in the medium also changes since it involves particles with modified properties. One is thus facing a coupled problem which has to be solved self-consistently. The method based on Green's functions (propagators) provides an ideal framework for solving the many-body problem using a self-consistent formulation as represented diagramatically in Fig. 1. Diagram 1(a) shows that the dressed SP propagator (thick line), which describes the propagation of a particle inside the medium, is obtained from the free propagator (thin line) and multiple iterations of the self-energy Σ. The self-energy contains all possible interactions of that particle with the medium. This is shown in graph 1(b) where the vertex function Γ, which acts as an effective interaction, collects all possible diagrams with four external points[18] and represents the coupling of the one-body propagator to the two-body propagator as indicated in Fig. 2.

Any approximation for Γ in the coupled set of equations of Fig. 1 determines a level of solution of the many-body problem which incorporates self-consistency. In the case of nucleons, the short-range nature of the nuclear interaction requires, as a minimum, the summation of the ladder diagrams shown in Fig. 3. These are the terms that renormalize the highly repulsive short-range part of the nuclear interaction V into a well behaved effective interaction Γ, which is the medium equivalent of the T matrix in scattering theory. The graphs in Fig. 3 can be written schematically as

$$\Gamma = V + Vgg\Gamma \equiv V + \Delta\Gamma \ , \tag{2.1}$$

where g is the one-body propagator. In terms of relative and total momenta, Eq. (2.1) reads

$$\begin{aligned}\langle \mathbf{k}_r|\Gamma(\mathbf{K},\Omega)|\mathbf{k}'_r\rangle &= \langle \mathbf{k}_r|V|\mathbf{k}'_r\rangle + \frac{1}{2}\int \frac{d^3q}{(2\pi)^3} i\int \frac{d\omega}{2\pi}[\langle \mathbf{k}_r|V|\mathbf{q}\rangle g(\tfrac{1}{2}\mathbf{K}+\mathbf{q},\Omega/2+\omega)g(\tfrac{1}{2}\mathbf{K}-\mathbf{q},\Omega/2-\omega)\langle \mathbf{q}|\Gamma(\mathbf{K},\Omega)|\mathbf{k}'_r\rangle] \\ &\equiv \langle \mathbf{k}_r|V|\mathbf{k}'_r\rangle + \langle \mathbf{k}_r|\Delta\Gamma(\mathbf{K},\Omega)|\mathbf{k}'_r\rangle \ ,\end{aligned} \tag{2.2}$$

where spin and isospin indices have been suppressed for simplicity, the matrix elements are antisymmetrized, and total momentum and energy conservation at each vertex has been taken into account. It should also be noted that the static nature of the basic interaction V implies that the ladder summed Γ depends on only one energy, Ω. Using identity (2.1) in diagram 1(b) one obtains the self-energy

$$\Sigma(\mathbf{k},\omega) = \int \frac{d^3k'}{(2\pi)^3}\int \frac{d\omega'}{2\pi i} e^{i\omega'\eta}\langle \mathbf{k}_r|V|\mathbf{k}_r\rangle g(\mathbf{k}',\omega') + \int \frac{d^3k'}{(2\pi)^3}\int \frac{d\omega'}{2\pi i}\langle \mathbf{k}_r|\Delta\Gamma(\mathbf{k}+\mathbf{k}',\omega+\omega')|\mathbf{k}_r\rangle g(\mathbf{k}',\omega') \ , \tag{2.3}$$

where $\mathbf{k}_r = (\mathbf{k}-\mathbf{k}')/2$.

A completely self-consistent solution of the many-body problem in the ladder approximation would require the solutio of Eq. (2.2) for the Γ effective interaction using the propagator g which solves the Dyson equation [graph 1(a)]

$$g(\mathbf{k},\omega) = \frac{1}{\omega - k^2/2m - \Sigma(\mathbf{k},\omega)} \tag{2.4}$$

in which the ladder contributions are included in the self-energy. Γ and g should then be used in Eq. (2.3) to determine the corresponding self-energy Σ and the Dyson equation (2.4) then has to provide the same propagator that was used to calculate Γ in Eq. (2.2). This nonlinear formulation has the same structure as the familiar Hartree-Fock problem but it is extended here to allow inclusion of dynamical correlations induced by ladder diagrams in this self-consistent scheme. As in the Hatree-Fock case an iterative solution method should be applied.

A. PPHH method: Particle-particle and hole-hole ladders

A first step towards the complete self-consistent solution to the problem illustrated in Fig. 1 was presented previously,[19,20] and is summarized here. The basic assumption is that self-consistency is only required for the most relevant energy ω in the self-energy, the quasiparticle energy

$$\varepsilon(\mathbf{k})=\frac{k^2}{2m}+\mathrm{Re}\Sigma(\mathbf{k},\varepsilon(\mathbf{k}))\ . \tag{2.5}$$

In this way one obtains propagators, $g_s^{(0)}$, which have the analytic structure of unperturbed propagators containing only a static SP potential $U(\mathbf{k})=\mathrm{Re}\Sigma(\mathbf{k},\varepsilon(\mathbf{k}))$ which accounts for the correlations of the system in an average way. In this simpler problem, the integral equation for the effective interaction Γ reads

$$\begin{aligned}\langle \mathbf{k}_r|\Gamma(\mathbf{K},\Omega)|\mathbf{k}_r'\rangle=\langle \mathbf{k}_r|V|\mathbf{k}_r'\rangle+\frac{1}{2}\int\frac{d^3q}{(2\pi)^3}\langle \mathbf{k}_r|V|\mathbf{q}\rangle\left[\frac{\theta_>(|\frac{1}{2}\mathbf{K}+\mathbf{q}|)\theta_>(|\frac{1}{2}\mathbf{K}-\mathbf{q}|)}{\Omega-\varepsilon(|\frac{1}{2}\mathbf{K}+\mathbf{q}|)-\varepsilon(|\frac{1}{2}\mathbf{K}-\mathbf{q}|)+i\eta}\right.\\ \left.-\frac{\theta_<(|\frac{1}{2}\mathbf{K}+\mathbf{q}|)\theta_<(|\frac{1}{2}\mathbf{K}-\mathbf{q}|)}{\Omega-\varepsilon(|\frac{1}{2}\mathbf{K}+\mathbf{q}|)-\varepsilon(|\frac{1}{2}\mathbf{K}-\mathbf{q}|)-i\eta}\right]\\ \times\langle \mathbf{q}|\Gamma(\mathbf{K},\Omega)|\mathbf{k}_r'\rangle\ ,\end{aligned} \tag{2.6}$$

where the step function $\theta_<(k)[\theta_>(k)]$ gives a nonvanishing contribution only if $k<k_F[k>k_F]$. The self-energy is given by

$$\begin{aligned}\Sigma(\mathbf{k},\omega)&=\Sigma^V(\mathbf{k},\omega)+\Sigma^{\downarrow}(\mathbf{k},\omega)+\Sigma^{\uparrow}(\mathbf{k},\omega)\\ &=\int\frac{d^3k'}{(2\pi)^3}\langle \mathbf{k}_r|V|\mathbf{k}_r\rangle\theta_<(k')+\int\frac{d^3k'}{(2\pi)^3}\langle \mathbf{k}_r|\Delta^{\downarrow}\Gamma(\mathbf{k}+\mathbf{k}',\omega+\varepsilon(k'))|\mathbf{k}_r\rangle\theta_<(k')\\ &\quad-\int\frac{d^3k'}{(2\pi)^3}\langle \mathbf{k}_r|\Delta^{\uparrow}\Gamma(\mathbf{k}+\mathbf{k}',\omega+\varepsilon(k'))|\mathbf{k}_r\rangle\theta_>(k')\ .\end{aligned} \tag{2.7}$$

This equation requires the separation of $\Delta\Gamma$ into two terms, $\Delta^{\downarrow}\Gamma$ and $\Delta^{\uparrow}\Gamma$, each having poles in one-half of the complex energy plane, which is achieved by means of a dispersion relation over the imaginary part.[19,20]

In this approximation the solution of the Dyson equation leads only to a shift in the SP energy according to Eq. (2.5). The Green's function expression for the binding energy

$$B=\frac{1}{2}\frac{4}{\rho}\int\frac{d\omega}{2\pi i}e^{i\omega\eta}\int\frac{d^3k}{(2\pi)^3}\left[\frac{k^2}{2m}+\omega\right]g(\mathbf{k},\omega)\ , \tag{2.8}$$

reduces to

$$B=\frac{1}{2}\frac{4}{\rho}\int\frac{d^3k}{(2\pi)^3}\left[\frac{k^2}{2m}+\varepsilon(\mathbf{k})\right]\theta_<(k) \tag{2.9}$$

where the factor 4 accounts for spin and isospin degeneracy.

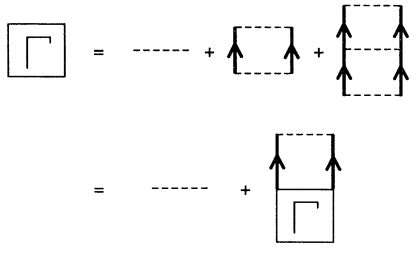

FIG. 3. Ladder approximation for the vertex function Γ.

It should be pointed out here that in the conventional Goldstone diagram expansion of the energy, the h-h self-energy contributions represent so-called off-shell contributions[32] which in that formulation do not contribute to the energy.[33] In the present self-consistent formulation the result (2.9) is very natural. It represents the energy which is obtained by solving the scheme of Fig. 1, where Γ is calculated in the ladder approximation of Fig. 3, and the Dyson equation is solved by keeping only the real on-shell self-energy contribution. As a result, the self-consistent propagator still has the structure of a free propagator. As such it is a simulation of the complete scheme of Fig. 1 in which the complete spectral distribution needs to be determined self-consistently. Due to the above approximation the spectral functions corresponding to the self-consistent SP propagator are still given by δ functions of strength 1 which are located at the quasiparticle energy and only results for the binding energy [Eq. (2.9)] will be presented.

B. DP method: Binding energy from the dressed propagator

In this section we use the complete dressed SP propagator in the determination of the binding energy. As described in Ref. 21, once the self-consistency at the level of the real on-shell self-energy [Eq. (2.5)] is achieved using the method described in the previous section, one can calculate the complete momentum and energy dependence of the self-energy from Eq. (2.7). The dressed propagator is then obtained by solving the Dyson equation. These

results are best expressed in terms of the spectral functions which show the fragmentation of SP strength in energy, as a contrast to the δ-function result characteristic of independent particle motion. This propagator can further be used as a first input to solve the complete ladder problem outlined at the beginning of this chapter. It is then possible to evaluate the energy directly from this dressed propagator according to Eq. (2.8). Moreover, by splitting Eq. (2.8) into

$$T=\frac{4}{\rho}\int\frac{d^3k}{(2\pi)^3}\frac{k^2}{2m}\int_{-\infty}^{\varepsilon_F}d\omega\, S_h(k,\omega) \tag{2.10}$$

and

$$\mathcal{V}=\frac{1}{2}\frac{4}{\rho}\int\frac{d^3k}{(2\pi)^3}\int_{-\infty}^{\varepsilon_F}d\omega\left[\omega-\frac{k^2}{2m}\right]S_h(k,\omega) \tag{2.11}$$

one can also give separate results for the kinetic and potential energies, respectively.

C. PP method: lowest order in Bethe-Brueckner expansion

For the purpose of later comparisons, we summarize here the Bethe-Brueckner expansion for the binding energy. This method is based on conventional time-independent perturbation theory. The Hamiltonian $\hat{H}=\hat{T}+\hat{V}$ is split into an exactly solvable problem, $\hat{H}_0=\hat{T}+\hat{U}$, and a perturbation $\hat{H}_1=\hat{V}-\hat{U}$, where the potential $\hat{U}$ is usually introduced in order to increase the rate of convergence of the series. The binding energy is given by the linked cluster expansion[1]

$$\begin{aligned}B&=T_0+E_c\\&=T_0+\left\langle\Phi_0\left|\sum_{n=0}^{\infty}\hat{V}\left[\frac{1}{E_0-\hat{H}_0}\hat{H}_1\right]^n\right|\Phi_0\right\rangle_l ,\end{aligned} \tag{2.12}$$

where T_0 is the free kinetic energy and E_0 the energy of the ground state $|\Phi_0\rangle$ of the unperturbed Hamiltonian $\hat{H}_0$. E_c is usually referred to as the correlation energy. The idea of the Bethe-Brueckner expansion is to rearrange the series (2.12) in such a way that the bare interaction V is replaced by a G matrix which, by grouping the selected class of p-p ladder diagrams to all orders in V, acts as a renormalized interaction between the nucleons. We note that the Bethe-Goldstone equation for the G matrix can be obtained from the Green's function Eq. (2.6) if one neglects the h-h propagating terms.

For the lowest order in the G matrix, the binding energy reads

$$B=T_0+\tfrac{1}{2}\sum_{k,j<k_F}\langle kj|G(\varepsilon(k)+\varepsilon(j))|kj\rangle . \tag{2.13}$$

The G matrix depends on the particular choice of the auxiliary potential. In the results presented here, we have used the continuous prescription introduced by Mahaux and collaborators[34,35]

$$U(k)=\sum_{j<k_F}\mathrm{Re}\langle kj|G(\varepsilon(k)+\varepsilon(j))|kj\rangle\quad\forall k . \tag{2.14}$$

In contrast to the standard choice which uses Eq. (2.14) only for $k<k_F$ and therefore yields a discontinuity at k_F, this prescription can be interpreted as an approximation to the physical mean field and, moreover, allows the consideration of those properties which are sensitive to particle-hole energy differences like, e.g., the effective mass, other than the binding energy. Using Eq. (2.14), and noting that the G matrix is real for energies $\Omega<2\varepsilon_F$, Eq. (2.13) reduces to

$$B=T_0+\tfrac{1}{2}\sum_{k<k_F}U(k) , \tag{2.15}$$

which is the Brueckner-Hartree-Fock (BHF) approximation to the binding energy.

D. GE method: Goldstone expansion for the kinetic and the potential energy

In this section we present a new method for calculating the binding energy of nuclear matter in terms of separate expansions for the kinetic energy T and the potential energy $\mathcal{V}$ of the correlated system

$$B=T+\mathcal{V} . \tag{2.16}$$

Although the formalism is based on Green's functions, we show below that the resulting expansion for the binding energy allows an interpretation in terms of Goldstone diagrams.

Given a two-body potential V in second quantization, the potential energy of nuclear matter reads

$$\mathcal{V}=\tfrac{1}{4}\sum_{k_1k_2k_3k_4}\langle\mathbf{k}_1\mathbf{k}_2|V|\mathbf{k}_3\mathbf{k}_4\rangle\langle\Psi_0|a_{k_1}^{\dagger}a_{k_2}^{\dagger}a_{k_4}a_{k_3}|\Psi_0\rangle . \tag{2.17}$$

Using the Lehmann representation for the two-body propagator g^{II} (defined with only two times) one can show that

$$\langle\Psi_0|a_{k_1}^{\dagger}a_{k_2}^{\dagger}a_{k_4}a_{k_3}|\Psi_0\rangle=-\frac{1}{\pi}\int_{-\infty}^{2\varepsilon_F}d\Omega\,\mathrm{Im}g^{II}(\mathbf{k}_3\mathbf{k}_4,\mathbf{k}_1\mathbf{k}_2;\Omega) . \tag{2.18}$$

The two-body propagator g^{II} obeys the equation shown schematically in Fig. 2. Assuming the SP propagators dressed in an average way by means of the real and energy-independent SP potential defined in Sec. II A, the algebraic expression for the pair of parallel lines in Fig. 2 is given by

$$\begin{aligned}&g_{(0)}^{II}(\mathbf{k}_3,\mathbf{k}_4,\mathbf{k}_1\mathbf{k}_2;\Omega)\\&\quad=(\delta_{k_1k_3}\delta_{k_2k_4}-\delta_{k_1k_4}\delta_{k_2k_3})\\&\qquad\times\left[\frac{\theta_>(k_1)\theta_>(k_2)}{\Omega-E_{12}+i\eta}-\frac{\theta_<(k_3)\theta_<(k_4)}{\Omega-E_{34}-i\eta}\right] ,\end{aligned} \tag{2.19}$$

where the notation $E_{ij}=\varepsilon(k_i)+\varepsilon(k_j)$ has been used. Multiplying the equation represented in Fig. 2 by V one gets

$$Vg^{II}=V(g^{II}_{(0)}+g^{II}_{(0)}\Gamma g^{II}_{(0)}) . \tag{2.20}$$

In the ladder approximation Γ obeys (see Fig. 3)

$$\Gamma=V+Vg^{II}_{(0)}\Gamma\equiv V+\Delta\Gamma , \tag{2.21}$$

and Eq. (2.20) can be written as

$$Vg^{II}=Vg^{II}_{(0)}+\Delta\Gamma g^{II}_{(0)} . \tag{2.22}$$

Inserting Eqs. (2.18), (2.22), and (2.19) in (2.17) one obtains

$$\mathcal{V}=\tfrac{1}{4}\sum_{k_1k_2k_3k_4}(\delta_{k_1k_3}\delta_{k_2k_4}-\delta_{k_1k_4}\delta_{k_2k_3}) \times\left[\mathrm{Im}\frac{-1}{\pi}\int_{-\infty}^{2\epsilon_F}d\Omega[\langle\mathbf{k}_1\mathbf{k}_2|V|\mathbf{k}_3\mathbf{k}_4\rangle+\langle\mathbf{k}_1\mathbf{k}_2|\Delta\Gamma(\Omega)|\mathbf{k}_3\mathbf{k}_4\rangle]\left[\frac{\theta_>(k_1)\theta_>(k_2)}{\Omega-E_{12}+i\eta}-\frac{\theta_<(k_3)\theta_<(k_4)}{\Omega-E_{34}-i\eta}\right]\right] . \tag{2.23}$$

It is readily seen that the term involving the V-matrix element inside the large square brackets of Eq. (2.23) represents the expectation value of the interaction with respect to the free Fermi sea ground state. Concerning the $\Delta\Gamma$ term, we first note that, by using dispersion relations,[19,20] $\Delta\Gamma$ can be divided into two pieces, $\Delta^{\downarrow}\Gamma$ and $\Delta^{\uparrow}\Gamma$. The term $\Delta^{\downarrow}\Gamma$ contains Goldstone diagrams of the type in Figs. 4(b), 4(c), 4(d), and 4(e) with pole structure in the lower half of the complex energy plane. Similarly, $\Delta^{\uparrow}\Gamma$ contains diagrams with poles in the upper half plane such as 4(f), 4(g), 4(h), and 4(i). Keeping in mind this separation, one realizes that the terms in Eq. (2.23) involving the real part of $\Delta\Gamma$ require the imaginary part (delta function) of the propagator, and one thus obtains the two terms $\mathrm{Re}\Delta^{\downarrow}\Gamma(\Omega=E_{34})\theta_<\theta_<$ and $\mathrm{Re}\Delta^{\uparrow}\Gamma(\Omega=E_{34})\theta_<\theta_<$ in schematic notation. On the other hand, the terms involving the imaginary part of $\Delta\Gamma$ require the real (principal) part of the propagator. Since $\Omega<2\epsilon_F$ over the range of integration, only $\mathrm{Im}\Delta^{\uparrow}\Gamma$ gives a contribution and, after using a dispersion relation for $\Delta\Gamma$, one can write the result as the sum of two terms $\mathrm{Re}\Delta^{\uparrow}\Gamma(\Omega=E_{12})\theta_>\theta_>$ and $-\mathrm{Re}\Delta^{\uparrow}\Gamma(\Omega=E_{34})\theta_<\theta_<$. Since the latter cancels exactly one of the contributions discussed above, Eq. (2.23) finally reads

$$\mathcal{V}=\tfrac{1}{4}\sum_{k_1k_2k_3k_4}(\delta_{k_1k_3}\delta_{k_2k_4}-\delta_{k_1k_4}\delta_{k_2k_3})[\langle\mathbf{k}_1\mathbf{k}_2|V|\mathbf{k}_3\mathbf{k}_4\rangle\theta_<(k_3)\theta_<(k_4)+\langle\mathbf{k}_1\mathbf{k}_2|\mathrm{Re}\Delta^{\downarrow}\Gamma(E_{34})|\mathbf{k}_3\mathbf{k}_4\rangle\theta_<(k_3)\theta_<(k_4) +\langle\mathbf{k}_1\mathbf{k}_2|\mathrm{Re}\Delta^{\uparrow}\Gamma(E_{12})|\mathbf{k}_3\mathbf{k}_4\rangle\theta_>(k_1)\theta_>(k_2)] . \tag{2.24}$$

The first term in Eq. (2.24) represents the expectation value of the interaction in the noninteracting ground state. It is represented by diagram (a) in Fig. 5, which is obtained by closing graph 4(a) with two hole lines. In a similar way, the second term in Eq. (2.24) is given by the infinite series of p-p and h-h ladder diagrams whose first terms are represented by graphs 5(b), 5(c), 5(d) and 5(e). They are obtained by closing diagrams 4(b), 4(c), 4(d) and 4(e) with two hole lines. Analogously, one obtains diagrams 5(f), 5(g), 5(h), and 5(i), contributing to the last term in Eq. (2.24), by closing graphs 4(f), 4(g), 4(h), and 4(i) with two particle lines.

It may appear that by including the identical diagrams 5(b) and 5(f) as well as [5(c), 5(h), 5(i)] and [5(g), 5(d), 5(e)], one runs into a multiple-counting problem. The origin of spurious-looking graphs in a Green's function expansion

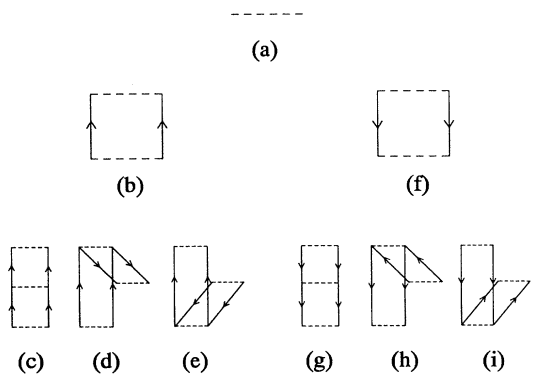

FIG. 4. Some low order Goldstone diagrams for the effective interaction Γ in the ladder approximation.

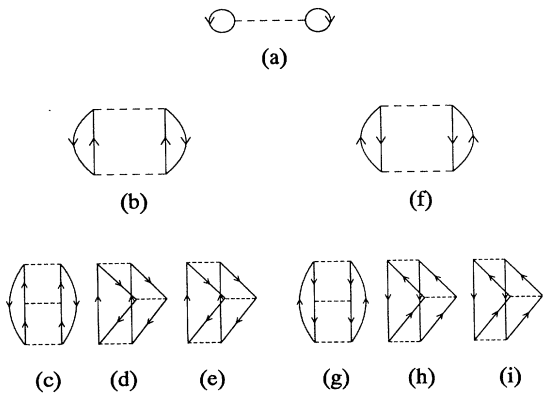

FIG. 5. Selected Goldstone diagrams for the potential energy $\mathcal{V}$ in the ladder approximation.

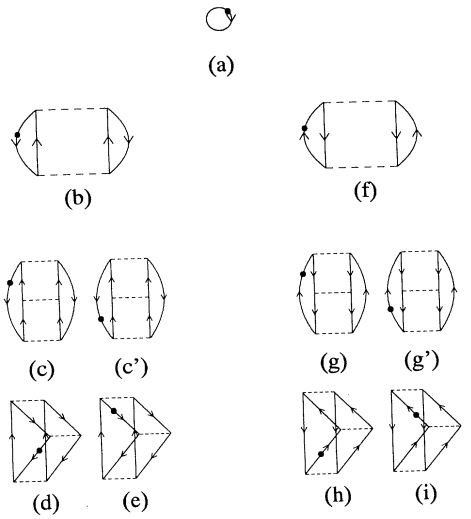

FIG. 6. Selected Goldstone diagrams for the kinetic energy T in the ladder approximation.

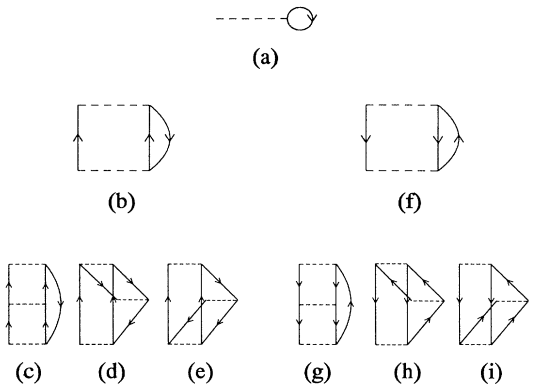

FIG. 7. Some Goldstone diagrams for the self-energy expansion in the ladder approximation.

for the potential energy was discussed by Mahaux and Sartor in Ref. 36. These authors show that each Goldstone term in the correlation energy E_c of the Bethe-Brueckner approach [Eq. (2.12)] appears as many times in the expansion for $\mathcal{V}$ [Eq. (2.16)] as the number of V-interactions contained in the diagram. Although their arguments were only made for p-p ladder diagrams, they also hold for diagrams involving p-p and h-h propagation, as is the case for the second-order diagrams 5(b) and 5(f), for the p-p third-border diagrams 5(c), 5(h), and 5(i), and the h-h third-order diagrams 5(g), 5(d), and 5(e). This can be extended and generalized to any order.

To obtain the binding energy, one also needs to know the kinetic energy at the same level of approximation as for the potential energy. One needs

$$T=\frac{4}{\rho}\int_0^\infty \frac{d^3k}{(2\pi)^3}\frac{k^2}{2m}n(k)\ , \tag{2.25}$$

where $n(k)$ is the momentum distribution of the correlated system. We will show below that by taking

$$n(k)=1+\left[\frac{\partial\Sigma^{\downarrow}(k,\omega)}{\partial\omega}\right]_{\omega=\varepsilon(k)},\quad k<k_F\ ,$$
$$n(k)=-\left[\frac{\partial\Sigma^{\uparrow}(k,\omega)}{\partial\omega}\right]_{\omega=\varepsilon(k)},\quad k>k_F \tag{2.26}$$

one generates order by order in V the kind of diagrams depicted in Fig. 6 for the kinetic energy expansion.[37,38] The derivatives in (2.26) are taken at the quasiparticle energy which ensures that the resulting momentum distributions are automatically real. Equations (2.26) do not represent exact results valid for all types of self-energy contributions. They do however, provide order by order the corrections to the momentum distribution which are generated by the ladder diagrams considered in this paper as will be shown below. Equations (2.26) can therefore also be used in the second order and BHF case (see, e.g., Ref. 39).

In the following second- and third-order examples, we show how one obtains the ladder corrections [diagrams 6(b), 6(c), 6(c'), 6(d),. . .] to the Fermi-gas momentum distribution [diagram 6(a)] from the derivative of the self-energy at the quasiparticle energy. The contributions $\Sigma^{\downarrow}(k,\omega)$ and $\Sigma^{\uparrow}(k,\omega)$ to the self-energy are taken from Ref. 21 and the corresponding second- and third-order diagrams are depicted in Fig. 7.

Consider the second-order correction to $n(k)$ for $k<k_F$ [diagram 6(b)]

$$\delta n^{(2)}(k)=-\frac{1}{2}\sum_{p_1p_2h_1}\frac{|\langle p_1p_2|V|kh_1\rangle|^2}{[\varepsilon(k)+\varepsilon(h_1)-\varepsilon(p_1)-\varepsilon(p_2)]^2}\ , \tag{2.27}$$

where, in what follows, p_i refers to a particle state ($p_i>k_F$) and h_i to a hole state ($h_i<k_F$). The corresponding second-order diagram for $\Sigma^{\downarrow}(k,\omega)$ [diagram 7(b)] reads

$$\Sigma^{\downarrow}_{(2)}(k,\omega)=\frac{1}{2}\sum_{p_1p_2h_1}\frac{|\langle p_1p_2|V|kh_1\rangle|^2}{\omega+\varepsilon(h_1)-\varepsilon(p_1)-\varepsilon(p_2)}\ , \tag{2.28}$$

whose derivative at $\omega=\varepsilon(k)$ is precisely the correction (2.27) to $n(k)$. Diagrams 6(c) and 6(c') read

$$\delta n^{(3,c)}(k)=-\frac{1}{4}\sum_{p_1p_2p_3p_4h_1}\frac{\langle h_1k|V|p_3p_4\rangle\langle p_3p_4|V|p_1p_2\rangle\langle p_1p_2|V|kh_1\rangle}{[\varepsilon(k)+\varepsilon(h_1)-\varepsilon(p_3)-\varepsilon(p_4)]^2[\varepsilon(k)+\varepsilon(h_1)-\varepsilon(p_1)-\varepsilon(p_2)]}\ , \tag{2.29}$$

$$\delta n^{(3,c')}(k)=-\frac{1}{4}\sum_{p_1p_2p_3p_4h_1}\frac{\langle h_1k|V|p_3p_4\rangle\langle p_3p_4|V|p_1p_2\rangle\langle p_1p_2|V|kh_1\rangle}{[\varepsilon(k)+\varepsilon(h_1)-\varepsilon(p_3)-\varepsilon(p_4)][\varepsilon(k)+\varepsilon(h_1)-\varepsilon(p_1)-\varepsilon(p_2)]^2}\ , \tag{2.29a'}$$

respectively. These are precisely the two terms that appear when performing the derivative at $\omega=\varepsilon(k)$ of the third-order self-energy diagram 7(c)

$$\Sigma^{\downarrow}_{(3,c)}(k,\omega)=\frac{1}{4}\sum_{p_1p_2p_3p_4h_1}\frac{\langle h_1k|V|p_3p_4\rangle\langle p_3p_4|V|p_1p_2\rangle\langle p_1p_2|V|kh_1\rangle}{[\omega+\varepsilon(h_1)-\varepsilon(p_3)-\varepsilon(p_4)][\omega+\varepsilon(h_1)-\varepsilon(p_1)-\varepsilon(p_2)]}\ . \tag{2.30}$$

The two contributions (2.29a) and (2.29a') to $n(k)$ correspond to the two possible time orderings in which the one-body operator, represented by the closed circle in Fig. 6, can be positioned in the hole line which is needed to close diagram 7(c). Since there is only one possible insertion for the third-order self-energy diagrams 7(d) and 7(e), each one gives only one contribution to $n(k)$ represented by graphs 6(d) and 6(e), respectively. The same analysis can be carried out for diagrams 6(f), 6(g), 6(g'), 6(h), and 6(i), which give the correction to $n(k)$ for $k>k_F$, and for any higher-order term. We therefore see that, order by order, the self-energy diagrams generate the different corrections to $n(k)$. By taking the derivative of the appropriate pieces of the self-energy [see Eq. (2.26)] calculated in the ladder approximation, one sums the complete series of p-p and h-h Goldstone diagrams for the kinetic-energy expansion. This result is a generalization of the calculation of the momentum distribution in Brueckner theory. Considering only p-p terms in the ladder equation leads only to diagrams 7(b) and 7(c) and as a result only diagrams 6(b), 6(c), and 6(c') are generated. Together with the higher-order ladder diagrams this leads to a depletion for momenta below k_F given by[40]

$$\delta n^{\mathrm{BHF}}(k)=-\frac{1}{2}\sum_{p_1p_2h_1}\frac{|\langle p_1p_2|G(\varepsilon(k)+\varepsilon(h_1))|kh_1\rangle|^2}{[\varepsilon(k)+\varepsilon(h_1)-\varepsilon(p_1)-\varepsilon(p_2)]^2}\ . \tag{2.31}$$

The corresponding contribution to the occupation of states above k_F is then obtained by considering the second-order self-energy diagram 7(f) with the V interactions replaced by G matrices. As a result one obtains for $k>k_F$

$$n^{\mathrm{BHF}}(k)=\frac{1}{2}\sum_{p_1h_1h_2}\frac{|\langle kp_1|G(\varepsilon(h_1)+\varepsilon(h_2))|h_1h_2\rangle|^2}{[\epsilon(h_1)+\varepsilon(h_2)-\varepsilon(k)-\varepsilon(p_1)]^2}\ . \tag{2.32}$$

III. RESULTS AND DISCUSSION

In this section we present the results for the momentum distribution and binding energy of nuclear matter for the v_2 central interaction derived from the Reid soft-core potential.[28]

A. Momentum distributions

The momentum distribution of nuclear matter has been calculated in two different ways. On the one hand, the hole spectral function $S_h(k,\omega)$ corresponding to the dressed SP propagator[21] introduced in Sec. II B determines the DP momentum distribution from

$$n(k)=\int_{-\infty}^{\varepsilon_F}S_h(k,\omega)d\omega\ . \tag{3.1}$$

On the other hand, Eq. (2.26) determines the GE momentum distribution as an expansion in terms of Goldstone p-p and h-h ladder diagrams, as discussed in Sec. II D. Results are shown in Fig. 8 at densities corresponding to $k_F=1.6$ and 1.8 fm^{-1}. The solid and dashed lines have been calculated from Eqs. (3.1) and (2.26), respectively. A particle-conserving approximation should fulfil the density sum rule

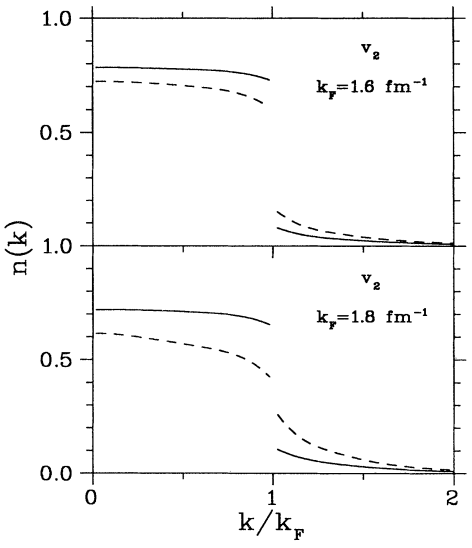

FIG. 8. Momentum distributions for the v_2 interaction at $k_F=1.6$ fm^{-1} and $k_F=1.8$ fm^{-1}. The solid line corresponds to the calculation using the (hole) spectral function [Eq. (3.1)] and the dashed line corresponds to the result of Eq. (2.26).

$$\frac{1}{\rho_0}\int_0^\infty \frac{4\,d^3k}{(2\pi)^3} n(k)=1\ , \tag{3.2}$$

where $\rho_0=2k_F^3/3\pi^2$ is the density of the uncorrelated system. In Table I we give results for the left-hand side of Eq. (3.2) for the two approximations to the momentum distribution at different densities. In the GE case the sum rule is fairly well fulfilled, whereas it is not completely reproduced in the DP case [see column (a) in Table I], especially at high densities. The reason is that the use of a non-self-consistent SP propagator in the DP calculation violates the Baym-Kadanoff conserving requirements,[41] according to which the number of particles is conserved if, for a given approximation to the two-body propagator g^{II} (see Fig. 2) the approximated SP propagator g satisfies the equations of Fig. 1. At present the vertex function Γ, used to obtain the dressed SP propagator g (see Fig. 1), has been determined from unperturbed propagators $g_s^{(0)}$ containing an average SP potential. Therefore, only when the ladder approximated Γ (see Fig. 3) is determined from the SP propagator which solves the equations of Fig. 1, i.e., when complete self-consistency is achieved, one fulfills the Bayn-Kadanoff requirement for the conservation of the number of particles

The tail of the momentum distribution as calculated from Eqs. (3.1) and (2.26) is shown in Figs. 9 and 10, respectively, at different densities. The parametrization

$$n(k)=\frac{k_F^5}{a}e^{-bk},\quad 2<k<4.5\ \text{fm}^{-1}\ , \tag{3.3}$$

has been suggested[40] recently for a separable representation of the Paris interaction, where $a=7$ fm^{-5} and $b=1.6$ fm. We obtain the same qualitative behavior between $k=2$ and 4.5 fm^{-1} but with different parameters. In the case of the momentum distribution calculated from the spectral function [Eq. (3.1) and Fig. 9] we obtain $a=12.8$ fm^{-5}, $b=1.45$ fm when results for all three densities ($k_F=1.6$, 1.8, and 2.0 fm^{-1}) are considered, whereas the values $a=12.6$ fm^{-5}, $b=1.47$ fm are obtained when only results for $k_F=1.6$ and 1.8 fm^{-1} are used.

The dispersion of results in the case of the momentum distribution calculated from the derivatives of the self-energy [Eq. (2.26) and Fig. 10] makes it difficult to assign a common parametrization for all densities, since we obtain $a=3.52$ fm^{-5}, $b=1.65$ fm when the three densities are used and $a=4.70$ fm^{-5}, $b=1.62$ fm if we only take results for $k_F=1.6$ and 1.8 fm^{-1}.

The differences between these results and those of Ref. 40 should only for a minor part be ascribed to the inclusion of the h-h correlations but rather to the essentially different interactions. In particular, important contributions between 2 and 4 fm^{-1} come from tensor correlations,[42] which are absent in our model potential. Also the short-range part of the interaction is not identical.

Results for $k^2n(k)$ and $k^4n(k)$ as functions of k are shown in Fig. 11. The function $k^4n(k)$ displays a maximum around $k=3$ fm^{-1} at all densities. This is different from the plateau behavior that was observed for the Paris interaction in Ref. 43. Although this difference can also be ascribed to the tensor interaction, we note that param-

TABLE I. Density sum rule for the potential v_2 at several densities. The notation GE corresponds to the momentum distribution calculated from Eq. (2.26) and DP to that calculated from Eq. (3.1). Columns (a), (b), and (c) represent different approximations for the DP momentum distribution as discussed in the text.

k_F (fm^{-1})	GE	DP (a)	DP (b)	DP (c)
1.6	1.0100	0.9670	0.9831	1.0000
1.8	1.0153	0.9402	0.9602	1.0000
2.0	1.0230	0.9018	0.9229	1.0000

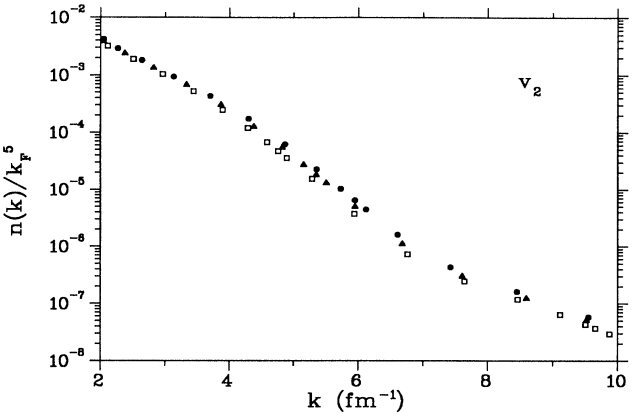

FIG. 9. Tail of the momentum distribution as calculated from Eq. (3.1) for the v_2 interaction at $k_F=1.6$ fm^{-1} (open squares), $k_F=1.8$ fm^{-1} (closed triangles), and $k_F=2.0$ fm^{-1} (closed circles).

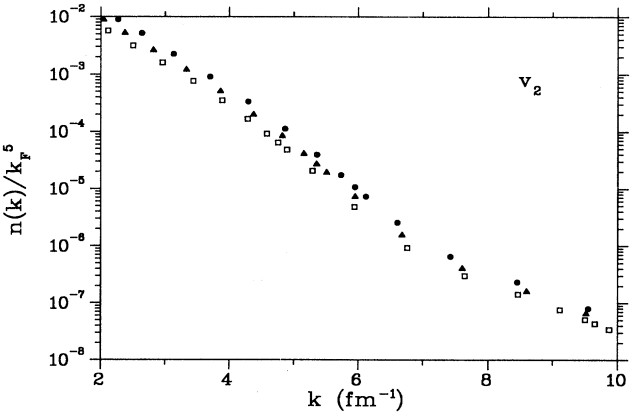

FIG. 10. Tail of the momentum distribution as calculated from Eq. (2.26) for the v_2 interaction at $k_F=1.6$ fm^{-1} (open squares), $k_F=1.8$ fm^{-1} (closed triangles), and $k_F=2.0$ fm^{-1} (closed circles).

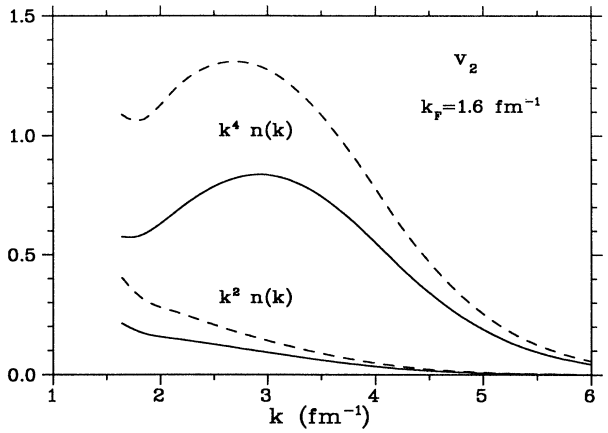

FIG. 11. Functions $k^2n(k)$ and $k^4n(k)$ for the v_2 potential at $k_F=1.6$ fm^{-1}. The solid and dashed lines correspond to the momentum distribution calculated from Eq. (3.1) and Eq. (2.26), respectively.

etrization given in Ref. 40 in the case of the Paris separable interaction leads to such a maximum located around 2.5 fm^{-1}.

An interesting result which can be deduced from these calculated momentum distributions (see Fig. 8) is the increasing depletion of the Fermi sea when the density increases. This seems to be in agreement with the intuitive notion that the particles will experience their mutual repulsion at shorter distance more frequently at higher density which results in an increase of high-momentum components in the ground state. As a consequence of this result a decrease of the discontinuity at k_F, the so-called z factor ($z(k_F)$), is obtained (see Table II) with increasing density. This should be contrasted with the results presented in Fig. 3 of Ref. 40, where the calculated z factor increases with density, up to a density corresponding to $k_F=1.7$ fm^{-1}. In principle, one expects that the smaller the density the more similar the system is to a free Fermi gas. The results of Ref. 40 seem to indicate the opposite behavior. At very low density one expects, nevertheless, that the z factor will go to 1 and as a consequence it seems that the Paris interaction gives a rather strong density dependence of this quantity when it is calculated in the BHF approximation using a continuous choice for the SP spectrum. Comparing to other results using other methods and interactions it could be concluded that this is a feature of the Paris potential. For the Paris interaction a value for $z(k_F)$ of 0.35 (Ref. 43) or 0.47 (Ref. 40) is obtained at normal density. A value of 0.7 (Ref. 44) is obtained for the Urbana v_{14} interaction[45] using the correlated basis function method. More recently, the same value of 0.7 has been obtained[46] for this same interaction although the total depletion is larger than in Ref. 44. The inclusion of the tensor force in the full Reid potential is expected to lead to a value closer to 0.7.[27]

TABLE II. Depletion ($n(0)$) and discontinuity at $k_F(z(k_F))$ of the momentum distribution for the potential v_2 at several densities. The notation GE corresponds to the momentum distribution calculated from Eq. (2.26) and DP to that calculated from Eq. (3.1).

k_F	$n(0)$		$z(k_F)$	
(fm^{-1})	DP	GE	DP	GE
1.6	0.78	0.72	0.63	0.41
1.8	0.72	0.61	0.52	0.09
2.0	0.65	0.49	0.41	−0.45

Further examination of Table II, indicates substantial differences between the DP and the GE estimates for $z(k_F)$, especially at higher density. In particular, the expansion in terms of Goldstone diagrams always predicts a smaller discontinuity and, if the density is pushed too far, it can even give an inverted discontinuity as is the case for $k_F=2.0$ fm^{-1}. This result suggests that the present approximation of the self-consistent problem of ladder and self-energy is breaking down. Indeed looking back at the way the ladder equation is solved in Eq. (2.6) this should hardly be surprising. The propagation of particles and holes is considered there with respect to a *free* Fermi sea, whereas the actually calculated momentum distribution shows an increasing deviation from this simple picture with increasing density. This problem would be remedied immediately when dressed SP propagators would be used to calculate the ladder equation [see Eq. (2.2)] since these propagators contain exactly the information on the probabilities for adding and removing particles from the correlated system. Clearly, the importance of this will increase with density and as a result the self-consistent solution using only an average SP energy insertion into the propagator has to break down. In our opinion it is very important to pursue the consequences of introducing the information on the modified Fermi surface into the ladder equation. Clearly, this has never been done before and it could lead to substantial differences in the density dependence of the effective interaction which might help to get a better understanding of the nuclear saturation problem.

B. Binding energy

Results for the binding energy obtained from the four approaches described in the previous section are shown in Fig. 12. The explicit values can be found in Table III. For comparison, we also include in Fig. 12 some other available nuclear matter results, namely, a variational Fermi hypernetted-chain calculation[30] and the hole-line calculation by Day.[22]

The PP results (long-dashed line with solid squares) correspond to the lowest order in the Bethe-Brueckner expansion discussed in Sec. II C [see Eqs. (2.15) and (2.14)]. The attraction associated with the use of a continuous SP spectrum is so large, relative to the two-hole line calculation by Day[22] with the standard discontinuous SP spectrum (dotted line with inverted solid triangles), that we do not obtain saturation. This result is important since it contradicts the conjecture that it is possible to get

TABLE III. Binding energy per particle in nuclear matter for the potential v_2 at several densities and for the different approximations described in the text. The PP results correspond to the lowest order in Bethe-Brueckner expansion with a continuous spectrum at k_F (Sec. II C), the PPHH results represent a simulation of the self-consistent ladder solution using a self-consistent quasiparticle energy (Sec. II A), the GE results correspond to an expansion in terms of Goldstone p-p and h-h diagrams (Sec. II D) and the DP results use the dressed SP propagator, although it is not yet self-consistent (Sec. II B). Rows (a), (b), and (c) correspond to different approximations for the DP momentum distribution, as discussed in the text.

k_F	PP	PPHH	GE			DP		
(fm^{-1})	(MeV)	(MeV)	T (MeV)	$\mathcal{V}$ (MeV)	B (MeV)	T (MeV)	$\mathcal{V}$ (MeV)	B (MeV)
1.6	−8.5	−4.0	73.1(67.5)	−78.9(−74.4)	−5.8(−6.9)	57.8	−64.7	−6.8 (a)
						67.8	−73.6	−5.8 (b)
						67.1	−73.6	−6.5 (c)
1.8	−13.8	−5.6	105.3(94.8)	−114.0(−106.1)	−8.6(−11.2)	73.8	−84.3	−10.5 (a)
						85.8	−94.9	−9.1 (b)
						92.1	−101.8	−9.7 (c)
2.0	−19.1	−5.5	152.4(133.5)	−158.2(−145.3)	−5.9(−11.8)	90.3	−102.2	−11.9 (a)
						105.7	−115.3	−9.5 (b)
						122.7	−132.3	−9.6 (c)

a reasonable approximation for the inclusion of three-body correlations by treating the two-hole-line approximation with a continuous choice for the SP spectrum. This has most recently been discussed in Ref. 40 and was originally proposed in Ref. 47. From the results obtained here one may conclude that this conjecture does not hold for any interaction.

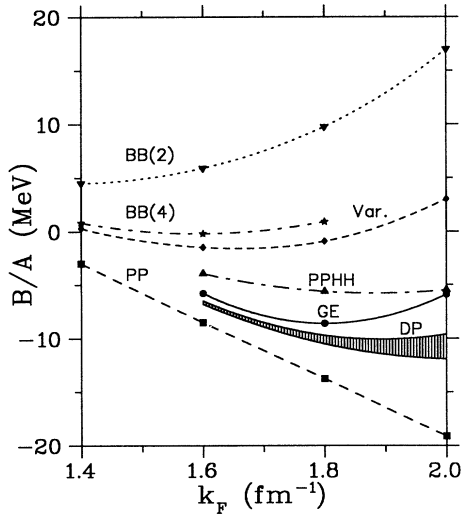

FIG. 12. Binding energy per particle in the case of the v_2 interaction for several approximations discussed in the text: the PP calculation (long dashed line with closed squares) described in Sec. II C, the PPHH calculation (long dash-dotted line with closed triangles) described in Sec. II A, the GE calculation (solid line with closed circles) described in Sec. II D and the DP calculation (hatching) described in Sec. II B. Day's results (Ref. 22) for the lowest order in the Brueckner expansion and for the 4-hole-line estimate using a discontinuous spectrum are represented by the dotted line with inverted closed triangles and the short dash-dotted line with closed asterisks, respectively. The short-dashed line with closed diamonds is the result for a variational upper bound calculation (Ref. 30) for the binding energy.

The results referred to as PPHH (long dash-dotted line with solid triangles) correspond to the method of Sec. II A [see Eq. (2.9)] which, in addition to the p-p ladders considered in the PP calculation, also adds to h-h ladders to all orders and intends to be a simulation of the complete self-consistent treatment of the problem illustrated in Fig. 1. We must note that, although expression (2.9) is formally identical to that used for the PP results [Eq. (2.15)], the SP spectrum $\varepsilon(k)$ in (2.9) contains the repulsive effects[21] that the h-h propagating terms in the effective interaction Γ [Eq. (2.6)] generate in the self-energy [Eq. (2.7)]. This effect is independent of the interaction used and, as a consequence, the binding energy obtained is more repulsive than the BHF prescription (PP results). Since the repulsion increases with the density this leads to a saturating effect in nuclear matter still at the level of two-body nonrelativistic interactions.[19,20] We recall that the propagators used in this first approach to the complete treatment still have the structure of noninteracting ones.

The two other calculations compared in this paper, namely, the GE method, containing infinite orders in h-h and p-p Goldstone ladder diagrams, and the DP method, which uses the dressed SP propagator, are new types of results never presented before. They are useful since they provide separate results for the kinetic and potential energy per particle of nuclear matter.

The results in parentheses in columns 4, 5, and 6 of Table III, corresponding to the GE calculation of Sec. II D, represent the kinetic, potential, and total binding energies when only momenta up to 4.5 fm^{-1} are considered. At $k_F = 1.6$ fm^{-1} for instance, this represents a factor 2.1 times the kinetic energy of the free Fermi gas T_0 whereas the total kinetic energy amounts to 2.3 times T_0. Although this last value is far from being the factor of 3 quoted in Ref. 40 for a crude extrapolation towards large momentum of the momentum distribution in the case of the Paris separable interaction at $k_F = 1.36$ fm^{-1}, the differences between the two values in column 4 are still large and show that a reliable value for the kinetic energy requires a careful calculation of the momentum

distribution for large momenta. We observe that it is necessary to go up to $k=7$ fm^{-1} to obtain an accuracy for the kinetic energy of 1% with respect to the total result.

Due to a compensation between the kinetic and potential energies at large k, these differences are smaller for the total binding energy (column 6 in Table III). However, they are important enough, especially at high density, to produce a sizable effect in the saturation point.

The GE binding energy is more repulsive than the BHF (PP) results. This is consistent with the discussion by Mahaux and Sartor in Ref. 36, where it shown that at the two-hole-line level one can expect more attraction when the energy is calculated as an approximation to the expectation value of the Hamiltonian in the correlated ground state than in lowest-order Brueckner theory, where one calculates the correlation energy, provided the SP potential is such that $U(h)<U(p)$. In the GE approach we have also included h-h propagation to all orders, in addition to the p-p forward-going diagrams discussed in Ref. 36, but the above feature is still found to be valid. The repulsion in the GE binding energy found for the v_2 interaction is due to the fact that the corresponding SP potential satisfies $U(h)>U(p)$. Any realistic interaction, however, leads to a SP potential such that $U(h)<U(p)$ and one should expect that the GE result, even if it contains h-h ladders to all orders, will lead to a more attractive binding energy per particle than the BHF (PP) results.

This is not in accord with the PPHH results discussed above and in Refs. 19 and 20, where a repulsive effect increasing with the density was associated with the inclusion of h-h correlations, independently of the two-body interaction used. The discussion above on the momentum distribution has already shown, however, that the concept of a SP energy used to dress SP propagators breaks down for too high density since it leads to an inversion of the occupation numbers at k_F. It was argued there that this breakdown can only be avoided by including a better description of the dressing of SP propagators into the calculation of the ladder interaction. One is then naturally led to the necessity of solving the problem of Fig. 1 in its full complexity. This means that the GE method would no longer be applicable since this requires simple particle or hole lines at most dressed by a SP energy. Only the energy obtained from Eqs. (2.10) and (2.11) would be relevant in that case. In comparison with this formulation the PPHH result is closest in spirit but can clearly not be considered definite.

The kinetic, potential, and binding energy results for the DP calculation of Sec. II B [see Eqs. (2.10) and (2.11)] are shown in columns 7, 8, and 9 [row (a)] of Table III, respectively. Rows (b) and (c) correspond to different manipulations of the momentum distribution, which are discussed below. A simple measure of the deviation from complete self-consistency is given by the density sum rule shown in column (a) of Table I. It is clear that the deviation from particle-number conservation is larger as the density increases. It is therefore premature to consider the results in row (a) of Table III as being representative of the completely self-consistent ones. As discussed above, only self-consistently dressed SP propagators fulfill the Baym-Kadanoff requirement[41] which will yield the conservation of the number of particles at each density. In addition, the most dramatic change in the result can be expected to occur when the ladder equation is solved using dressed propagators.

In order to investigate how the fulfillment of the density sum rule (3.2) influences the binding energy, we have considered two different adjustments of the momentum distribution. First, we have considered an exponential fit to $n(k)$ in a zone where an exponential law is observed (from $k\simeq 2$ fm^{-1} to $k\simeq 3.5$ fm^{-1} at all densities). We extrapolate this behavior to all higher momenta even if, as shown in Fig. 9, the exponential law is no longer valid. At each k, the corresponding hole spectral function $S_h(k,\omega)$ is multiplied by an overall factor to reproduce the new modified $n(k)$. The density sum rule and energy results are given in column (b) of Table I and row (b) of Table III, respectively. Second, $n(k)$ has been modified assuming that the final self-consistent $n(k)$ will lie somewhere between GE results [Eq. (2.26) and dashed line in Fig. 8] and the DP results [Eq. (3.1) and solid line in Fig. 8]. We determine a factor that brings the momentum distribution DP at the origin $[n(k=0)]$ half way between the DP and the GE value, and this factor is used to renormalize the momentum distribution for $k<k_F$. The remaining momentum distribution $(k>k_F)$ is multiplied by the required factor which ensures particle-number conservation. The hole spectral functions $S_h(k,\omega)$ are also renormalized accordingly to reproduce the new modified $n(k)$. In this way, by removing some occupation below k_F and introducing some occupation above k_F we obtain a momentum distribution in between the DP and GE estimates. The results are given in column (c) of Table I and row (c) of Table III.

We should emphasize that the models (b) and (c) are not meant to represent the final self-consistent momentum distribution, but a simple way to anticipate what one can expect for a calculation using the dressed propagator with a good fulfillment of the sum rule, as we expect to be the case when the SP propagator is determined self-consistently. When comparing with the bare results (a), we observe a repulsive effect in the binding energy, which is more important for the higher densities where the density sum rule was reproduced worse. Since, due to the use of a not self-consistent propagator, the DP results must be considered as preliminary and rather uncertain, we have represented them by a hatching including both the original result (a), which violates the density sum rule, and the result (c), in which the momentum distribution $n(k)$ has been adjusted so as to reproduce the sum rule. We observe a repulsion in the binding energy when compared to the PP (BHF) result. Although this repulsion is not as spectacular as that obtained with the PPHH method, which was meant to represent a simulation of the fully self-consistent DP calculation, we still observe that the saturation density is moved to considerably lower densities. We believe that this is a genuine effect of the inclusion of h-h correlations.

A comparison with Day's four-hole-line estimate[22] shows that the results presented here give somewhat

more binding. This result can probably be related to the observation that the results depend sensitively on the treatment of the SP spectrum and the resulting coherence that can be generated by the ladder equation. This quantum coherence is considerably enhanced with the inclusion of h-h propagation to all orders. It should be remembered that the ladder equation (with h-h propagation to all orders) can display the same kind of coherence and instabilities (pairing in this case) as the particle-hole random-phase approximation. In the conventional hole-line expansion with a gap in the SP spectrum this possible coherence is relegated to high order in the number of hole lines and can never be recovered in practice. For the same reasons it cannot be expected to give adequate results for such a collective phenomenon as pairing. In contrast, a self-consistent formulation as advocated throughout this paper incorporates a description of pairing.[24] In addition it can ultimately incorporate a self-consistent treatment of depletion effects.

The h-h correlations have also been investigated within a model space approach (MBHF)[48,49] resulting in an increase of the binding energy per nucleon and a decrease of the saturation density for realistic interactions. Recently, Mahaux and Sartor suggested[50] that the SP spectrum used in the MBHF approach left uncanceled part of the third-order hole-bubble diagram, which is largely repulsive. This motivated a reinvestigation of the MBHF approach[51] in which the standard BHF spectrum was taken for holes and the MBHF spectrum for particles and, although the binding energy is substantially decreased with respect to the previous result, the saturation density is practically the same, which is smaller than that obtained with a BHF calculation where only p-p correlations are considered. When comparing this last MBHF result (curve labeled Ring-BM in Fig. 1 of Ref. 51) with the BHF calculation using a continuous SP spectrum (curve labeled BHF-C) one observes that beyond $k_F = 1.25$ fm^{-1} the Ring-BM binding energy is more repulsive than the BHF-C and, since this repulsion increases with the density, it yields a smaller saturation density. This is precisely the effect that we quoted in Ref. 20 for the PPHH calculation, also reported in the present work, and seems to be as well the trend of the complete ladder approach (DP results), although for the latter it is necessary to have a self-consistent propagator before drawing definite conclusions.

IV. SUMMARY AND CONCLUSIONS

In this work we have compared results for the binding energy of nuclear matter from different prescriptions based on Green's functions formalism, namely, (i) the familiar BHF approximation using a continuous SP spectrum (PP method), (ii) an approach, based on a self-consistent formulation for the SP propagator with the inclusion of p-p and h-h correlations, which leads to a self-consistent on-shell SP energy (PPHH method), (iii) an estimate using the completely dressed (but not yet self-consistent) propagator (DP method) and (iv) an expansion in terms of Goldstone p-p and h-h ladder diagrams (GE method). The results have been obtained for the central v_2 interaction which is derived from the Reid soft-core potential.

The GE calculation provides also results for the momentum distribution in nuclear matter. The expansion can be summed by taking the derivative of the self-energy at the quasiparticle energy and leads to a $n(k)$ which conserves the number of particles. Another estimate of the momentum distribution has also been given in terms of the hole spectral function corresponding to the dressed propagator obtained in the DP calculation. In this case, particle number is partially violated, especially at high densities, due to the use of propagator which is not fully self-consistent. However, the qualitative behavior is similar to that obtained from the expansion GE and to other predictions of $n(k)$ for realistic interactions.[44,43,46,40] It is shown that the simple procedure of including a SP energy to simulate the effect of correlations breaks down at higher density since the calculated momentum distribution for the v_2 interaction gives a higher occupation for momenta just above k_F than for momenta just below.

The PPHH binding energy, which includes the h-h correlations to all orders using an average SP propagator and is intended to be a simulation of the completely self-consistent coupled ladder self-energy problem, is more repulsive than the PP result which only includes p-p ladders. This effect increases with the density giving rise to a lower saturation density as was noted in a previous paper.[20]

A lower saturation density has also been observed here for the DP calculation, although the repulsion for the binding energy with respect to a Brueckner-type calculation (PP results) is substantially less than that predicted by the PPHH results. However, the lack of self-consistency for the SP propagator leads to particle number violation and one should be cautious before drawing definite conclusions.

The Goldstone p-p and h-h ladder diagrams summed in the GE calculation give a binding energy which is rather dependent on the shape of the auxiliary SP potential used. In the case of the v_2 interaction discussed here, for which $U(h) > U(p)$, a more repulsive binding energy and a lower saturation density are obtained.

Although there are other indications that one can obtain a lower saturation density when the h-h correlations are included,[48,49,51] their effects will lie more clearly established once the methods addressed in the present work have been applied to a realistic interaction with proper treatment of the pairing instabilities intrinsic in the symmetric treatment of particles and holes.[24,25] Work along these lines is in progress.[27]

It is important to note that the nuclear saturation problem has to be readdressed since new experimental results from $(e,e'p)$ reactions indicate a substantial [about 20–25 % (Ref. 15)] depletion of shell model orbitals. Since relativistic calculations will provide only minor depletion effects[13] the relativistic results for nuclear saturation have to be regarded with reservation. In addition it has been shown that strong collective correlations exists in the $^3S_1$-$^3D_1$ channel which have not been considered appropriately up to now and are the result of a uniform

treatment of particles and holes.[26] It has also been argued here that a great inconsistency is present in the treatment of Pauli corrections in the ladder equation since they are considered with respect to a free Fermi sea whereas the actually calculated momentum distributions show an increasing deviation of the Fermi sea picture with increasing density. To determine the relevance of the h-h correlations in the saturation problem, it is therefore crucial to solve the ladder approximation in terms of self-consistently dressed propagators which take the correct Pauli effects into account. This formulation will include a proper treatment of depletion since it dresses the particles with the complete off-shell energy dependence of the self-energy and therefore leaves no ambiguity for the choice of the auxiliary potential. It also is able to give a consistent treatment of quantum coherence at the level of p-p and h-h correlation since the ladder equation has similar features as the conventional ph-RPA. As a result pairing will be automatically included in this scheme. It is therefore hoped that such a complete treatment will shed new light on the old problem of nuclear saturation with the new ingredient that the calculations should also lead to a sizable depletion of mean field SP states. Additional studies of the influence of long-range ph correlations and three-body forces are then still necessary but at least an unambiguous result for the influence of short-range correlations on the nuclear saturation problem will have been established.

ACKNOWLEDGMENTS

This research was supported by CAYCIT Grant No. PB89-0332 (Spain) and by the Condensed Matter Theory Program of the division of Materials Research of the U.S. National Science Foundation under Grant No. DMR-9002863 (at Washington University) which also provided computer time for the calculations which were performed at the Pittsburgh Supercomputer Center. Additional support was provided by NATO under Grant No. RG 85/0684.

[1]H. A. Bethe, Annu. Rev. Nucl. Sci. **21**, 93 (1971).
[2]B. D. Day, Rev. Mod. Phys. **39**, 719 (1967).
[3]A. D. Jackson, Annu. Rev. Nucl. Part. Sci. **33**, 105 (1983).
[4]V. R. Pandharipande and R. B. Wiringa, Rev. Mod. Phys. **51**, 821 (1979).
[5]J. W. Clark, Prog. Part. Nucl. Phys. **2**, 89 (1979).
[6]H. Kümmel, K. H. Lührmann, and J. G. Zabolitzky, Phys. Rep. **36**, 1 (1978).
[7]D. M. Ceperley and M. H. Kalos, in *Monte Carlo Methods in Statistical Mechanics,* edited by K. Binder (Springer Verlag, New York, 1979).
[8]M. R. Anastasio, L. S. Celenza, W. S. Pong, and C. M. Shakin, Phys. Rep. **100**, 327 (1983).
[9]R. Brockmann and R. Machleidt, Phys. Lett. **149B**, 283 (1984).
[10]B. ter Haar and R. Malfliet, Phys. Rep. **149**, 207 (1987).
[11]C. Horowitz and B. D. Serot, Nucl. Phys. **A464**, 613 (1987).
[12]H. Müther, R. Machleidt, and R. Brockmann, Phys. Lett. B **198**, 45 (1987).
[13]M. Jaminon and C. Mahaux, Phys. Rev. C **41**, 697 (1990).
[14]P. K. A. de Witt Huberts, J. Phys. G **16**, 507 (1990).
[15]G. van der Steenhoven, private communication.
[16]J. Carlson, V. R. Pandharipande, and R. B. Wiringa, Nucl. Phys. **A401**, 49 (1983).
[17]P. Grangé, A. Lejeune, M. Martzolff, and J. F. Mathiot, Phys. Rev. C **40**, 1040 (1989).
[18]A. A. Abrikosov, L. P. Gorkov, and I. E. Dzyaloshinsky, *Methods of Quantum Field Theory in Statistical Physics* (Dover, New York, 1975).
[19]A. Ramos, A. Polls, and W. H. Dickhoff, *Condensed Matter Theories,* edited by J. S. Arponen, R. F. Bishop, and M. Mannienen (Plenum, New York, 1988), Vol. 3.
[20]A. Ramos, W. H. Dickhoff, and A. Polls, Phys. Lett. B **219**, 15 (1989).
[21]A. Ramos, A. Polls, and W. H. Dickhoff, Nucl. Phys. **A503**, 1 (1989).
[22]B. D. Day, Phys. Rev. C **24**, 1203 (1981).
[23]L. P. Kadanoff and G. Baym, *Quantum Statistical Mechanics* (Benjamin, New York, 1962).
[24]W. H. Dickhoff, Phys. Lett. B **210**, 15 (1988).
[25]W. H. Dickhoff, in *Condensed Matter Theories,* edited by J. Keller (Plenum, New York, 1989), Vol. 4, p. 271.
[26]B. E. Vonderfecht, C. C. Gearhart, W. H. Dickhoff, A. Polls, and A. Ramos, Phys. Lett. B **253**, 1 (1991).
[27]B. E. Vonderfecht, W. H. Dickhoff, A. Ramos, and A. Polls, work in progress.
[28]R. V. Reid, Ann. Phys. (N.Y.) **50**, 411 (1968).
[29]D. Ceperley, G. V. Chester, and M. H. Kalos, Phys. Rev. B **16**, 3081 (1977).
[30]K. E. Schmidt and V. R. Pandharipande, Nucl. Phys. **A328**, 240 (1979).
[31]T. T. S. Kuo, Z. Y. Ma, and R. Vinh Mau, Phys. Rev. C **33**, 717 (1986).
[32]B. H. Brandow, Rev. Mod. Phys. **39**, 771 (1967).
[33]C. A. Engelbrecht and H. A. Weidenmüller, Nucl. Phys. **A184**, 385 (1972).
[34]J. Hüfner and C. Mahaux, Ann. Phys. (N.Y.) **73**, 525 (1972).
[35]J. P. Jeukenne, A. Lejeune, and C. Mahaux, Phys. Rep. **25C**, 83 (1976).
[36]C. Mahaux and R. Sartor, Phys. Rev. C **19**, 229 (1979).
[37]B. H. Brandow, Phys. Rev. **152**, 863 (1966).
[38]D. J. Thouless, *The Quantum Mechanics of Many-Body Systems* (Academic, New York, 1961).
[39]C. Mahaux, P. F. Bortignon, R. A. Broglia, and C. H. Dasso, Phys. Rep. C **120**, 1 (1985).
[40]M. Baldo, I. Bombaci, G. Giansiracusa, U. Lombardo, C. Mahaux, and R. Sartor, Phys. Rev. C **41**, 1748 (1990).
[41]G. Baym and L. P. Kadanoff, Phys. Rev. **124**, 287 (1961).
[42]J. G. Zabolitzky and W. Ey, Phys. Lett. **76B**, 527 (1978).
[43]P. Grangé, J. Cugnon, and A. Lejeune, Nucl. Phys. **A473**, 365 (1987).
[44]S. Fantoni and V. R. Pandharipande, Nucl. Phys. **A427**, 473 (1984).
[45]I. E. Lagaris and V. R. Pandharipande, Nucl. Phys. **A359**, 331 (1981).
[46]O. Benhar, A. Fabrocini, and S. Fantoni, Phys. Rev. C **41**, R24 (1990).

[47]C. Mahaux, Nucl. Phys. **A328**, 24 (1979).
[48]H. Q. Song, S. D. Yang, and T. T. S. Kuo, Nucl. Phys. **A462**, 491 (1987).
[49]M. F. Jiang, T. T. S. Kuo, and H. Müther, Phys. Rev. C **38**, 2408 (1988).
[50]C. Mahaux and R. Sartor, Phys. Rev. C **40**, 1833 (1989).
[51]M. F. Jiang, T. T. S. Kuo, and H. Müther, Phys. Rev. C **40**, 1836 (1989).